CrossMark

TECHNICAL ARTICLE

Evaluation of a coal seam roof water inrush: case study in the Wangjialing coal mine, China

Yifan Zeng[1,2] · Qiang Wu[1] · Shouqiang Liu[1] · Yanliang Zhai[3] · Huiqing Lian[2] ·
Wei Zhang[4]

Abstract The Wangjialing Mine in southern Shanxi Province is seriously threatened by roof water and is infamous for a water inrush disaster that happened there in 2010. A root-cause-analysis was conducted. Three key issues, the height of the mining-induced fractured zone in formations overlying the coal seam, the water yield of aquifers overlying the coal seam, and working face water inflows before and after pretreatment of roof water-bearing aquifers, were studied based on the "three maps–two predictions" approach. According to the multi-source information composite principle, abundance zoning maps of the roof aquifer were made using the overlapping function of geographic information system (GIS) for five controlling factors: aquifer thickness, total core recovery, drilling fluid quantity, permeability, and thickness of brittle and plastic strata. Borehole-specific data from in-situ pumping tests were used to verify the water abundance results. For areas that did not meet the verification requirements, the weights of the controlling factors were calibrated by reestablishing the analytic hierarchy process judgment matrix. The total height of the fractured zone within the #2 coal seam roof was calculated using an empirical formula. An established roof crack safety zoning map was used to evaluate that aspect. A three-dimensional numerical simulation of the groundwater flow system was established based on the site conceptual model of the roof aquifer and was used to predict the working face inflows. The results indicated that the 20,518 working face of the 205 panel had the greatest abundance of water.

✉ Yifan Zeng
   zengyifan_1011@sina.com

   Yanliang Zhai
   zhaiyanliang2009@163.com

   Wei Zhang
   zw19890616@gmail.com

1 National Engineering Research Center of Coal Mine Water Hazard Control, China University of Mining and Technology, Beijing 100083, China

2 Hebei State Key Laboratory of Mine Disaster Prevention, North China Institute of Science and Technology, Beijing 101601, Yanjiao, China

3 The 4th Geological Team of Hebei Geology and Mining Bureau, Chengde 067000, China

4 Northwest Nonferrous Survey Engineering Co. Ltd., Xi'an 710054, China

Introduction

Three measures were taken to optimize the coal industrial structure in China. First, the construction of large coal production bases has been promoted. In 2015, the total annual production of the 14 large coal bases reached 3.123 billion tons, accounting for more than 90% of the country's output (State Council of the PRC 2014). Second, large coal companies have been developing at an incredible speed. The total annual output of the nine largest has reached 1.5 billion tons, accounting for 38.9% of the China's total production. Each of these companies has an annual output of more than a hundred million tons (State Council of the PRC 2016). Third, coal production has been improved

by sharply reducing the number of mines from 25,000 (in 2005) to 11,000 (in 2014), whereas the number of large mines increased from 290 (in 2005) to 970 (in 2014). Of the large coal mines, 54 are 10 million ton mines, with a total annual output of nearly 700 million tons, accounting for 18% of the nation's output (State Council of the PRC 2014). Also, more and more of these large coal companies now use intelligent fully-mechanized mining equipment, increasing the number of coal seam failures and the transformation and destruction of roof aquifers.

In the last decade, the impact of roof water damage has become increasingly problematic (Dong 2007; Wu 1995, 2014). On August 17, 2007, the Shandong Huayuan mine had a roof water inrush that left 181 miners dead; the cumulative water output was 6.22 million m^3. On March 28, 2010, a serious inrush accident in the Wangjialing mine trapped 153 people, resulting in an 8-day rescue effort that saved all but 38 miners. On May 30, 2011, the Shanxi Ningtiaota mine had a roof inrush accident; the water inflow was 1200 m^3/h for months. Thus, analyzing inrush mechanisms, forecasting roof water inrush, and formulating preventive and control measures in advance are very important to ensure safe production and improve mining efficiency.

Research outside of China on water inrush from aquifers overlying coal seams mainly involve mining under waterbodies (Booth 1986; Hu and Wang 1997). The former Soviet Union required that such mines must determine a site-specific safe depth for each mine in conformance with the regulations (Hill and Price 1983; Wu et al. 2013). Japan requires 100 m coal pillars for mining under the sea (Islam et al. 2009), while the British, for the same conditions, uses room-and-pillar mining in shallow areas (at depths of at least 61 m below the sea bottom) and longwall technology in deeper mines (at depths of at least 105 m; Booth and Bertsch 1999; Kim et al. 1997). The maximum mining thickness is 1.7 m.

Roof water hazard prediction has generally focused on the abundance of water in roof aquifers and the inrush mechanisms. The representative forecasting methods include the "three top layers" theory (Booth et al. 2000; Rauch 1989; Singh and Kendorski 1981), "key stratum" theory (Qian et al. 1996; Xu and Qian 2000), mutation theory pan-decision analysis, and the "two zones" study (Xu et al. 2011; Zeng et al. 2016a). However, where roof aquicludes are thin or non-existent, or the fractured zone encompasses the entire overburden aquifer(s), evaluating water abundance is challenging. Furthermore, because of the deep exploration levels and limited pumping tests in most coal mining regions in China, it is difficult to accurately evaluate the true distribution of an aquifer's water yield properties. In addition, previous studies that used a theoretically reasonable and GIS-based water-richness

index lack on-site verification and correction of the aquifer's water abundance (Liu and Yang 2006; Liu et al. 2006). To overcome these problems and improve overall accuracy and credibility, we used an explorative "verification and correction method" in which the evaluation results were verified or calibrated by limited but available unit-inflow data from pumping tests. Based on the "three map–two predictions" technology from GIS, we studied the height of the fractured zone, aquifer water yield, zoning evaluation of roof water inrush risk, and working face water inflow predictions before and after roof aquifer pretreatment in the Wangjialing mine, making use of the mine's rich observational data and addressing three key issues: the roof water source, pathway, and strength.

Geological and hydrogeological conditions

The Wangjialing mine is a large modern facility constructed by the China Coal Group in Xiangning County, Shanxi Province. It is part of the Hedong Coalfield, located within the eastern Ordos Basin, and covers an area of 119.71 km^2 (Fig. 1). The coal-bearing strata form a monocline structure striking northwest (dip angle 3° to 10°) with excellent coal seam conditions and enormous reserves. The reserves of the main coal seams (#2, #3, and #10) are estimated at 1.495 billion tons. Coal seams #2 and #10 are thick, stable, and of good quality. Mine construction was completed in September 2012 and production began. Systematical resource and hydrogeological exploration have been conducted and the mine's layout has been largely completed. A large amount of data are available on overlying strata movement during mining and roof water inrush evaluations.

According to outcrops and drilling data, the formations are classified from old to new into the: Fengfeng Group of Middle Ordovician, Benxi Group of Middle Carboniferous, Taiyuan Group of Upper Carboniferous, Shanxi Group of Lower Permian, Xiashihezi Group of Lower Permian, Upper Xiashihezi Group of Late Permian, Shiqianfeng Group of Late Permian, and Liujiagou Group of Lower Triassic, Neogene, and Quaternary. The overall geological structure of the coalfield is a monocline, striking northeast and dipping to the northwest, accompanied by small folds. The dip angle is generally gentle, mainly 3°–5°, though occasionally up to 10°. There are 49 faults reported, with seven visible on the ground surface and 42 faults identified by surface geophysics. The throws of 18 of the faults are greater than or equal to 5 m, whereas the throws of the other 31 faults are less than 5 m. The main coal-bearing strata are the Shanxi Group of the Lower Permian and the Taiyuan Group of the Upper Carboniferous. The average thickness of these two strata is 87.7 m, including 13 coal
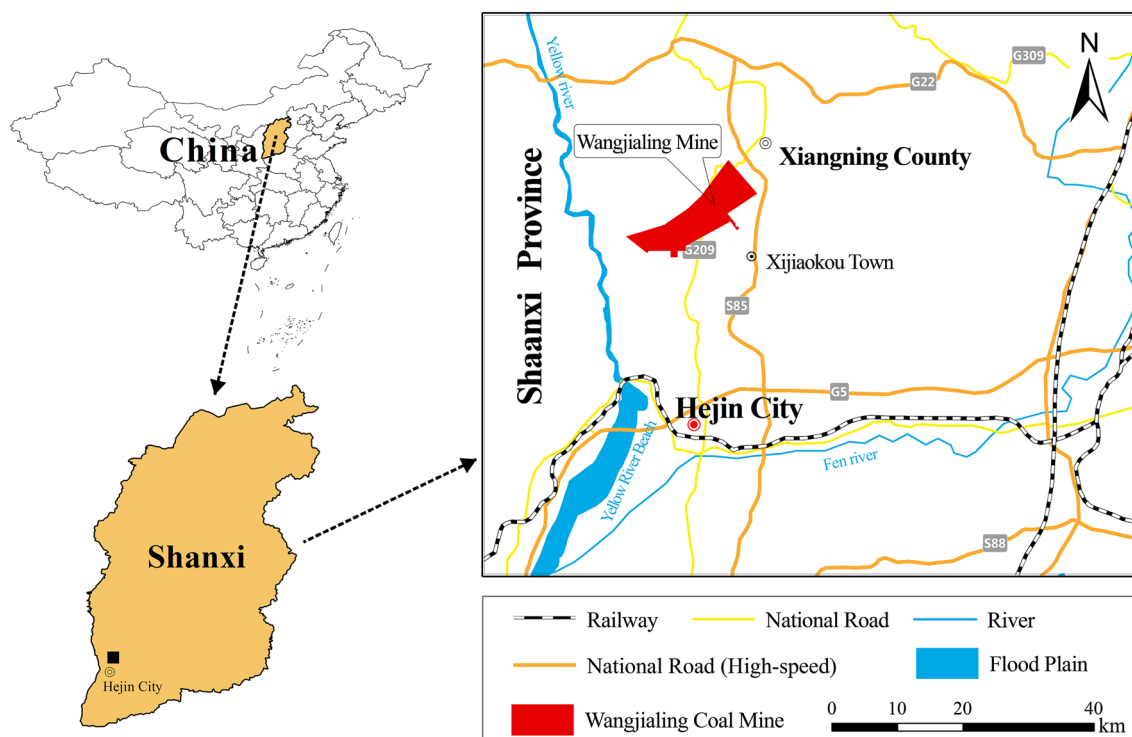
Fig. 1 Location of the study area

seams with a total thickness of 11.5 m and a coal bearing ratio of 11.3%. There are three main commercial coal seams, whose average thickness is 10.4 m and mineable coal-beating coefficient is 11.8%. Faults with displacements less than 5 m can influence mine faces, but have no effect on rationally dividing mining areas, while faults with displacements greater than 5 m also affect these.

The #2 coal seam of the Wangjialing mine is in the middle and lower part of the Shanxi Formation, with thicknesses ranging from 2.98 to 7.80 m and an average thickness of 6.11 m. It contains a clay band and a simple structure. The clay band is approximately 0.20 m thick, and the coal seam thins from southwest to northeast. The roof consists mostly of sandstone and sandy mudstone. The coal seam floor is composed of siltstone and mudstone, fine-grained sandstone, and quartz sandstone. The recoverable area of this coal seam is 116.64 km^2, accounting for 97.4% of the total mine. The main aquifers are: Quaternary loose-rock porous aquifers, a fractured Permian sandstone aquifer, a fractured Carboniferous Taiyuan limestone (karst) aquifer, and a fractured Middle Ordovician karst aquifer group (Fig. 2). The thick Permian sandstone aquifer is the main threat to safely mining the #2 seam.

The fractured Permian sandstone aquifer is mainly composed of the K10 sandstone at the bottom of the upper Shihezi Formation, K9 sandstone at the middle of the Lower Shihezi Formation, K8 sandstone at the bottom of the

Lower Shihezi Formation, and K7 sandstone at the base of the Shanxi Formation. The #2 coal roof aquifers include the K8, K9, and K10 fractured sandstone aquifers. The total sandstone thickness of the roof ranges between 2.2 and 89.6 m, with an average of 48.63 m (Fig. 3). According to pumping test data, the water inflow from a single hole in this aquifer ranges from 0.014 to 2.38 L s, while inflow ranges from 0.0002 to 0.058 L (s m). The calculated permeability coefficient ranges from 0.0007 to 0.2207 m/day and the water level elevation is from 818.5 to 1051.1 m above mean sea level. The burial depth of this weak aquifer gradually deepens from south to north and from east to west. Water level elevation of the sandstone is from 650 to 1100 m. The water level is higher in the northeastern part and lowest in the western part of the mine. The groundwater flows from the southeast to the northwest and turns westward in the western part of the field.

Assessment principle of coal seam roof water inrush

The "three maps–two predictions" method for evaluating the risk of roof water rock burst was developed as a practical step to address mine flooding in northern China (Wu 2002). It addresses three main problems in evaluating the likelihood of roof rock bursts: water sources overlying the coal seam, water pathways, and water inflow intensity. "Three maps" refers to maps that: (1) demarcate the coal
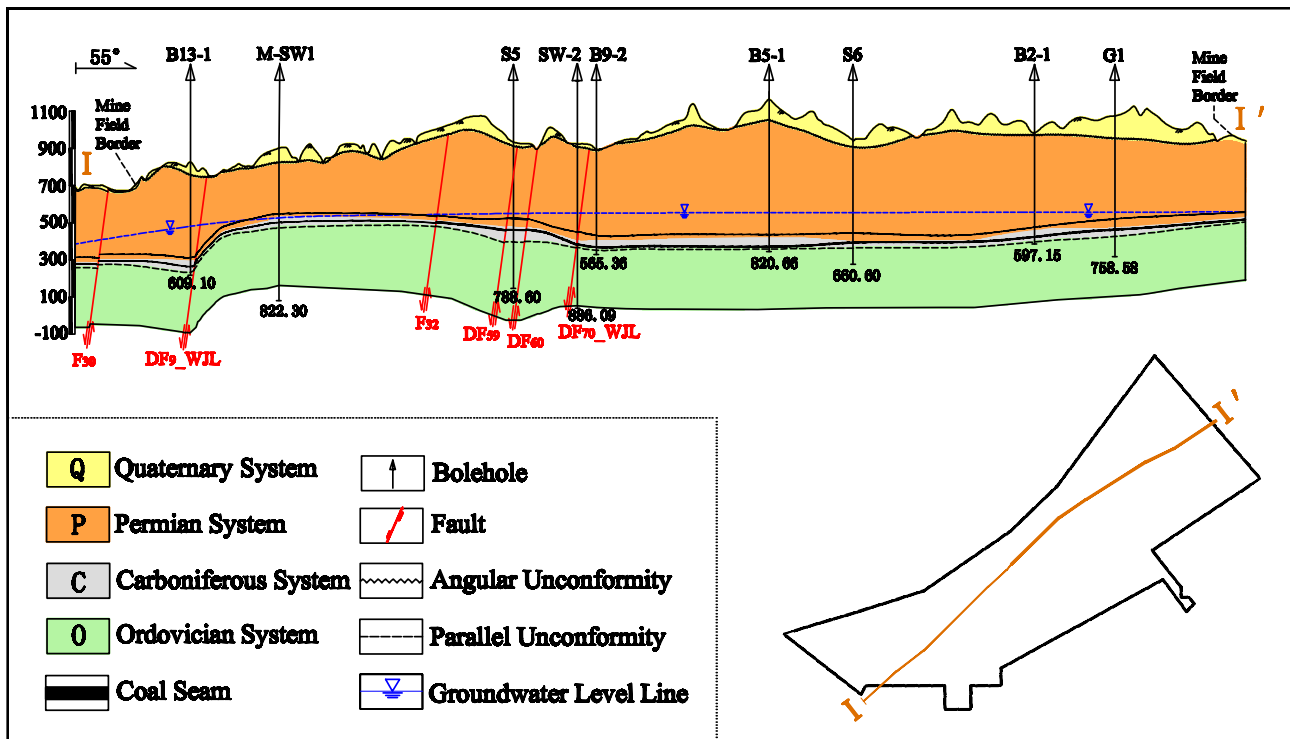
Fig. 2 Geological cross-section at Wangjialing Mine

roof aquifer based on saturation, (2) indicate the extent of roof fractures, and (3) analyze the potential areas where a roof rock burst could occur. "Two predictions" involves segmenting the working face and predicting overall water inflow before and after the roof aquifer is grouted (Wu et al. 2015a).

The method has inspired systematic research and made it possible to evaluate the risk of water inrush through the roof. This only occurs when the mining-induced, water-conductive, fractured roof zone is hydraulically connected to the overlying aquifer and when this aquifer remains full even when water begins to leak through cracks in the roof near the working face.

The crack safety zoning map shows if the roof thickness is greater than the thickness of the fractured zone; if the fractures are not connected to the aquifer, and then this area is defined as relatively safe. If the fractures extend beyond the thickness of the roof, and connect to the aquifer, then this area has a greater risk of an inrush.

The collected hydrogeological data of the study area was used to determine the main factors controlling the water yield index, which was constructed using the multi-source information fusion technology of GIS (Wu and Zhou 2008). All of the normalized sub-thematic maps were superimposed using GIS software, and then the relative importance (weight) of each controlling factor was calculated for every overlapping area. This allowed us to partition the study area based on the relative water yield strength of the aquifer.

A comprehensive water inrush (inflow) zoning map is built by overlapping the coal seam roof aquifer water abundance map onto the crack safety map. Its theoretical basis is that when the fractured zone penetrates the aquifer and connects to areas with abundant water, considerable water inflow occurs. Otherwise, the area is relatively safe. This is also the core concept of "three maps–two predictions" method (Wu and Wang 2006).

Based on this hydrogeological conceptual model, a three-dimensional numerical simulation model was constructed using the advanced international professional software, Visual Modflow (Wu et al. 2015a). After the model was calibrated using relevant hydrological data, the advanced Zone Budget function in Visual Modflow was used to predict regional water inflow at the working face when periodic working face pressure occurs.

Risk assessment of coal seam roof water inrush

Coal seam roof zone safety evaluation

The goaf generated as the coal is mined changes the stress in the surrounding rock. When the stress in the surrounding rock exceeds the compressive, tensile, or shear strength, the

Fig. 3 The simplified distribution map of aquifers and coal seams

Stratigraphic Age		Rock name (Thickness/m)	Stratigraphic Column	Distance (m)
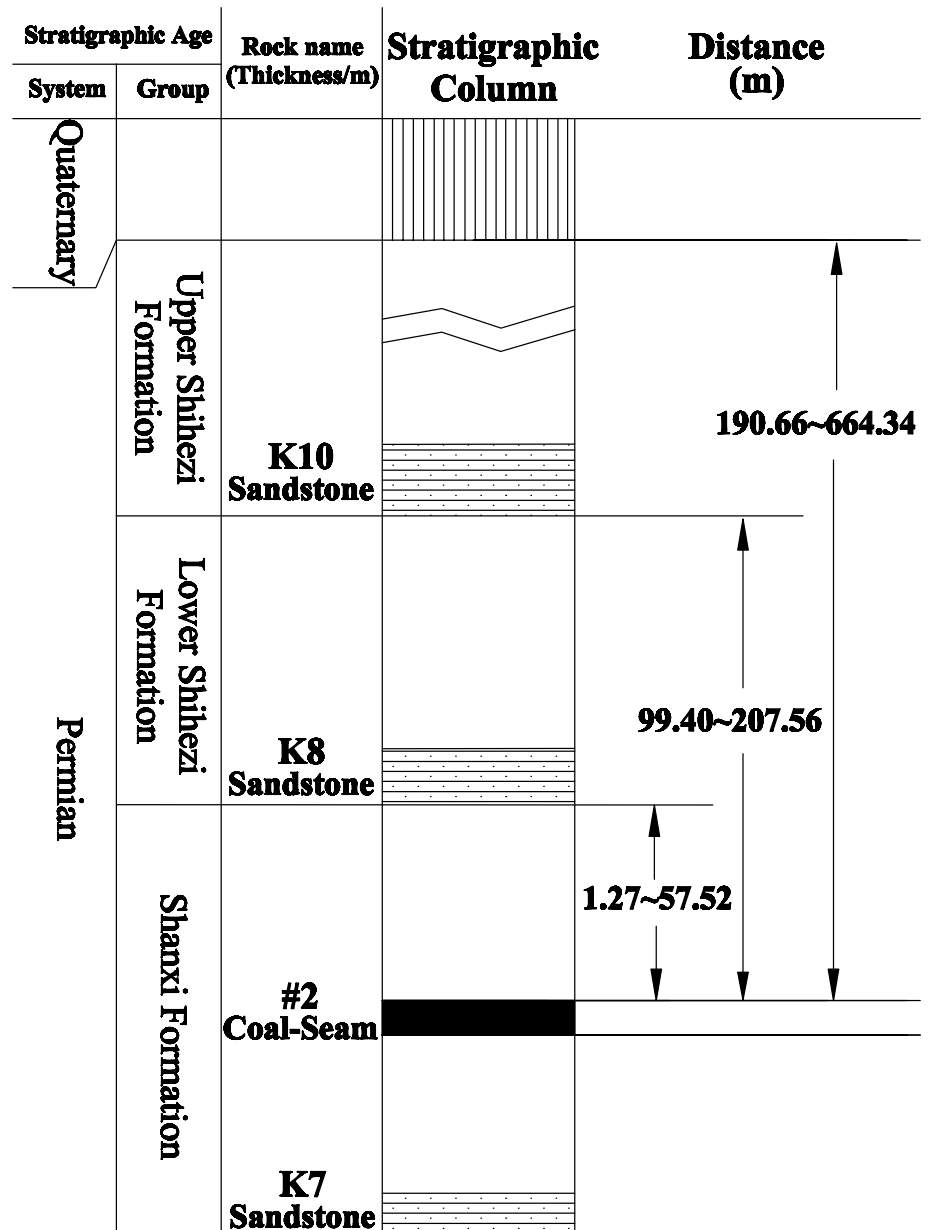
surrounding rock fractures and can even collapse (Xu et al. 2016). Depending on how mining damages the overburden, the roof strata can normally be divided into three zones, from bottom to top: caving zone, fissured zone, and bending zone. Because the #2 coal seam of the mine has not yet been exploited on a large scale, the height of these three zones is not readily available. The uniaxial compressive strength of the saturated roof rock ranges from 20 to 50 MPa. In general, the lithology can be defined as medium hard rock. The height of the #2 coal seam fractured zone can be calculated with Eq. (1) (Wu and Wang 2006), as expressed below:

$$H_{li} = \frac{100M}{0.26M + 6.88} + 11.49 \qquad (1)$$

where H_{li} = the fractured zone and M = the thickness of the coal seam, both in m.

the fractured zone formed after the coal seam is mined is shown in Fig. 4. The relationship between the fractured zone and roof aquifer is revealed by comparing the developing height with the thickness of the overlying confining bed. Because the fractured zone formed after the #2 coal seam is exploited has developed into the overlying Permian sandstone aquifer, the whole area has to be regarded as relatively dangerous (Supplemental Fig. 1).
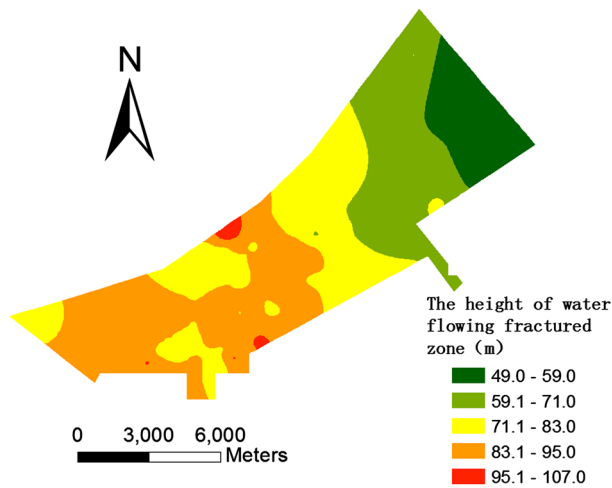
Fig. 4 Thematic map of the height of water flowing fractured zone after #2 coal seam mining

Coal seam roof aquifer water abundance evaluation

Determine the main factors controlling aquifer water abundance and establish thematic maps

Based on our study of the geological and hydrogeological conditions, five factors were used to evaluate the water abundance of the #2 coal roof aquifer: (1) the combined thickness of the aquifers, (2) the recovery ratio of core, (3) the drilling fluid quantity, (4) the ratio of the thickness of brittle and plastic rock, and (5) the permeability coefficient.

The combined thickness of the aquifers (the thin, medium, and coarse sandstones in the #2 coal roof, the K10 aquifers, and the fractured aquifer) in the Permian sandstone is important because it generally correlates with the water yield of the aquifers, if other factors are unchanged. Based on the borehole data, the authors used the interpolation function of Surfer and the spatial analysis function of ArcGIS to produce a thematic map of the thickness of the Permian sandstone aquifer. From Supplemental Fig. 2a, it can be seen that the sandstone thickness varies from less than 20 m in the central and eastern areas to more than 70 m in the west.

The ratio of the length of the core that is retrieved relative to the length drilled is an indicator of the rock mass integrity and the extent to which rock fissures intersect. Less core recovery means that the rock is more broken or more intensively fractured, which generally results in stronger water yield from the corresponding aquifer. From Supplemental Fig. 2b, it can be seen that the total core recovery gradually increased from northwest to southeast, reaching its maximum in the south-central part of this study area where the recovery ratio exceeded 90%.

The amount of drilling fluid required can reflect karst features or fracture development, which in turn reflect the permeability of the strata and likely its abilities to store and transmit water. Therefore, the greater the amount of drilling fluid, the stronger the water yield of the aquifer. A thematic map (Supplemental Fig. 2c) of the drilling fluid data shows that relatively large quantities were used in the north-central part of the study area, while relatively small quantities were needed in the southeast.

The thickness ratio of brittle and plastic rock can be used to qualitatively estimate aquifer permeability. Rocks with different mechanical properties fracture differently when stressed. Brittle sandstone releases stress by fracturing, so its permeability is greatly enhanced. Plastic argillaceous rock releases stress by plastic deformation, so its permeability changes little. In general, the larger the ratio, the more permeable the aquifer will be. The thematic map of this ratio (Supplemental Fig. 2d) indicates the ratio is relatively large in a small area of the southern part of the mine area, with a value more than 5.0, while the ratio elsewhere is much smaller, generally below 1.7.

The permeability coefficient is the seepage velocity when the pressure gradient is equal to 1. When the pressure gradient is constant, the larger the permeability coefficient, the greater the seepage velocity. When the seepage velocity is constant, the larger the permeability coefficient, the smaller the pressure gradient. So the permeability coefficient quantitatively represents the transmissivity of the rock strata. Therefore, to some extent, the permeability coefficient reflects the water yield of the aquifer. The authors have mapped the permeability coefficient (Supplemental Fig. 2e) based on mine pumping test results. It can be seen that the permeability coefficient gradually increases from south to north, reaching 0.19 m/day in the northeastern part of the mine from less than 0.09 m/day in the southern and central-southern part.

Determine the weight of each controlling factor

The analytic hierarchy process (AHP) is a multi-criterion decision analysis (evaluation) method that views a complex multi-objective decision-making problem as a stratified system, ranking and organizing the multiple levels of objectives or criteria so that each element of the system, except for the top one, is subordinate to one or more other elements. It is a simple, flexible, and practical method developed by Thomas L. Saaty (Wu et al. 2015b; Zeng et al. 2016b) and an effective way to convert semi-qualitative and semi-quantitative problems into quantitative ones.

The AHP model can be divided into three levels by analyzing the factors influencing the water yield of the aquifer. Since evaluating the water yield is the goal, it becomes the A-level (target level) of the AHP structural model. The

seepage field, aquifer, and lithology all affect the aquifer's water yield, and their influence needs to be reflected by their related sub-factors, so they are regarded as the B-level (sub-criteria). Sub-factors constitute the C-level (decision making level). In this way, the decision problem can be analyzed (Fig. 5).

By constructing a judgment matrix and comparing every two factors that affect the water yield, the relative importance of each factor is ranked, and values representing their importance are assigned a numerical ranking from 1 to 9 and the reciprocal scaling proposed by Saaty (Wu et al. 2015b; Zeng et al. 2016b). Table 1 presents the calculated weights of the controlling factors after the matrix operations.

Building the water yield index model

In order to comprehensively consider the influence of the geo-information on the aquifer's water yield, we need to integrate all of it. To make all the geoscience information comparable, we firstly apply a dimensionless method to all the collected data. Equation (2) is used to normalize the data of each influencing factor.

$$A_i = a + \frac{(b - a) \times (x_i - \min(x_i))}{\max(x_i) - \min(x_i)} \quad (2)$$

where A_i is the dimensionless data; a and b are the minimum and maximum values within the normalized range;

Table 1 Weighting of the controlling factors

| Controlling factor	Aquifer thickness (W_1)	Core recovery ratio (W_2)	Drilling fluid quantity (W_3)	Ratio of brittle and plastic rock (W_4)	Permeability coefficient (W_5)
Weighting	0.1976	0.1040	0.1635	0.2079	0.3270

x_i is the raw data; and min (x_i) and max (x_i) respectively represent the minimum and maximum values. The thematic maps of the controlling factors are merged after normalization, and a new database is thus generated.

After overlapping all of the normalized geological information based on the weights of controlling factors, the "water yield index" is calculated. The water yield index value reflects the relative water yield of the aquifer and can be represented as follows:

$$CI = \sum_{k=1}^{n} W_k * f_k(x, y) \quad (3)$$

where CI = the water yield index; n = the number of controlling factors considered, which is 5 in this paper; K = the sequence number of factors; W_k = the weight of the kth controlling factor; $f_k(x, y)$ = the normalized value of the kth controlling factor; and x and y are coordinates. Then, the

Fig. 5 The AHP model of the water yield property of the aquifer
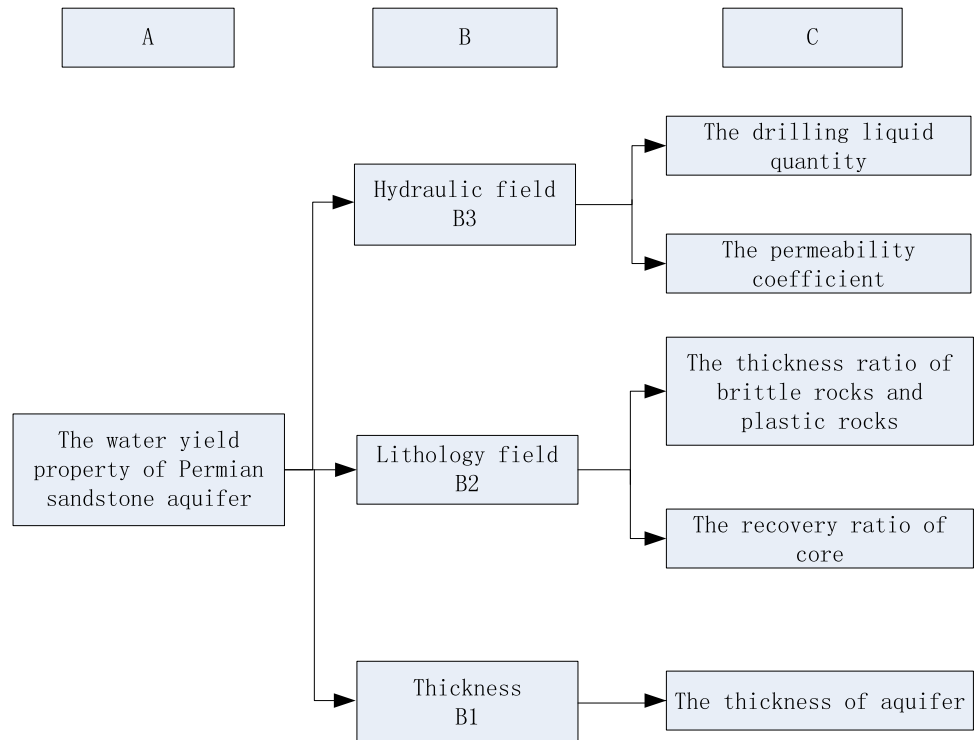
model evaluating the water yield of the #2 coal seam roof Permian sandstone aquifer is expressed as:

$$CI = \sum_{k=1}^{5} W_k * f_k(x, y) = 0.1976 f_1(x, y) + 0.1040 f_2(x, y)$$
$$+ 0.2079 f_3(x, y) + 0.327 f_4(x, y) + 0.1635 f_5(x, y) \quad (4)$$

Aquifer water yield evaluation

The water yield index of the #2 roof aquifer was calculated using this model. To facilitate the application during production, the whole area was divided into five sub-regions with different levels of water abundance. The zoning map of water abundance is shown in Fig. 6 based on the partitioning thresholds of 0.123, 0.172, 0.237, and 0.331, as determined by natural breaks (Wu and Wang 2006). Such a result needs to be verified or corrected to be sure of its accuracy and should only be considered to be reasonable once it is verified. Otherwise, the parameters involved in the water abundance index evaluation model need to be adjusted or the weights of the controlling factors have to be recalculated until the zoning results meets the demand.

In this study, the evaluation zoning result was tested by using the measured borehole units-inflow data. First, using the measured data, the thematic map of the units-inflow was built with GIS technology (Fig. 7) and compared with the thematic map of water abundance. Second, seven representative measurements of inflow data were chosen to verify the water abundance zoning results (Table 2). It can be seen that after the evaluation zoning results were corrected, the trend within the final zoning result was consistent with that of the water inflow map. The inflow data from these seven hydrogeological drill holes all passed the verification
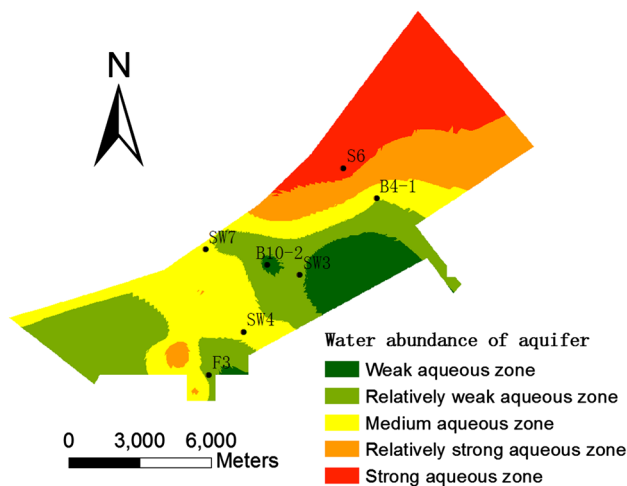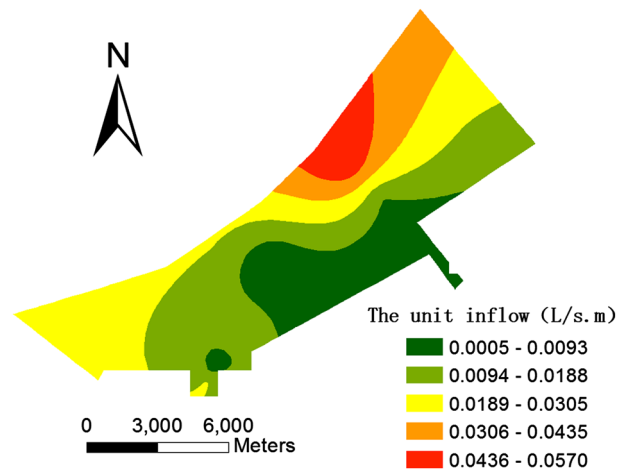

Fig. 7 Thematic map of the units inflow

test, which suggests that the zoning result is reasonable and reflects the water abundance of the aquifer.

Coal seam roof water inrush risk evaluation

After overlapping the water abundance zoning map of the roof aquifers with the crack safety zoning map using Arc-GIS, we considered geological structure to produce a comprehensive assessment zoning map of water inflow (inrush) for the roof sandstone aquifers (Fig. 8).

To facilitate its application, areas where caving fails to occur are deemed to be relative safe. Areas where caving develops are considered to be riskier, and five risk levels are defined: dangerous, relatively hazardous, transition zone, relatively safe, and safe. It can be seen from Fig. 8 that the area the north of borehole S6 has a higher risk of roof water inrush, while the south central area to the southeast of borehole SW3 has less risk of an inrush. The reason that the area north of borehole S6 is more likely to suffer roof water inrush is that the permeability of the aquifer is higher there, while factors such as the thickness of the sandstone, total core recovery, and the brittle-plasticity ratio are intermediate, which causes a relative strong water yield index, and perhaps most important, the fractured zone formed after mining in this area reaches the overlying aquifer.

Mines water inflow prediction

As discussed earlier, a three-dimensional hydrogeological model was developed using Modflow groundwater simulation software. The amount of water inflow (inrush) from the 20,518 working face within the 205 mining area was predicted based on the comprehensive zoning map of water inflow risk. The 20,518 working face, which is 3 km in

Fig. 6 Zoning map of water abundance of the aquifer overlying coal seam #2

Table 2 Verification of the water-filling aquifer's water-richness partition

Borehole number	Inflow	Area in division of water enrichment of aquifer map	Satisfaction of sequential verification
S6	0.058	Strong	Yes
SW7	0.0199	Medium	Yes
SW4	0.015	Medium	Yes
B4-1	0.0103	Medium	Yes
F3	0.005	Relatively weak	Yes
SW3	0.0048	Relatively weak	Yes
B10-2	0.0002	Weak	Yes
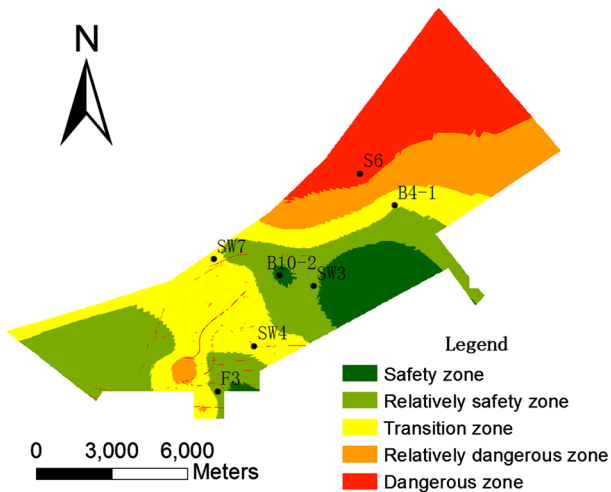
Fig. 8 Zoning of water inrush risk

length and 0.3 km in width, is located in the northeast part of the mine, within an area classified as dangerous with respect to a roof water risk inrush.

Model establishment

The water levels in the main aquifers in the study area are not closely related to levels of precipitation or the phreatic aquifers, though data is limited. The area's hydrogeology can be divided into layers; from top to bottom, they are the: Quaternary Holocene alluvial and fluvial porosity aquifers; aquitard between the Quaternary and Permian sandstone aquifers; Permian sandstone fracture aquifer group consisting of K8, K9, and K10 aquifer group; and the impermeable layer between the Carboniferous Taiyuan aquifer and Permian K8 aquifers.

Long-term, high-frequency water level and water volume data are very important for model calibration. Although the data collected in the Wangjialing mine do not meet these requirements, the available data can still

be regarded as valid and the model can be regarded as acceptable as long as the test and the regulation of hydrological parameters of the model are reasonably replicated. In this study, the model was calibrated using S6 hole pumping test data (Fig. 9).

Dynamic prediction of water inflow

Because of changing pressures, we divided the 205 mining area every 15 m as the working face moves forward to predict the dynamic water inflow and the change regularity of the 20,518 working face. The Zone Budget module in Modflow was used to divide the 20,518 working faces into 51 stages to make predictions (Fig. 10). In areas with abundant water, as the coal mining face advances, the overlying roof rock bends down and cracks, so that water inflow increases as the permeability of the aquifer becomes larger. However, when the overlying roof strata falls, the original fractures are compacted and closed, and then water inflow decreases as the permeability coefficient of the aquifer becomes smaller. The trend of water inflow changes along with the advancement distance (periodic pressure) of the coal mining face.

Conclusions

The "water-rich index" method was used to evaluate the relative risk of a roof water inrush in the Wangjialing coal mine. Based on an analysis of the basic data within
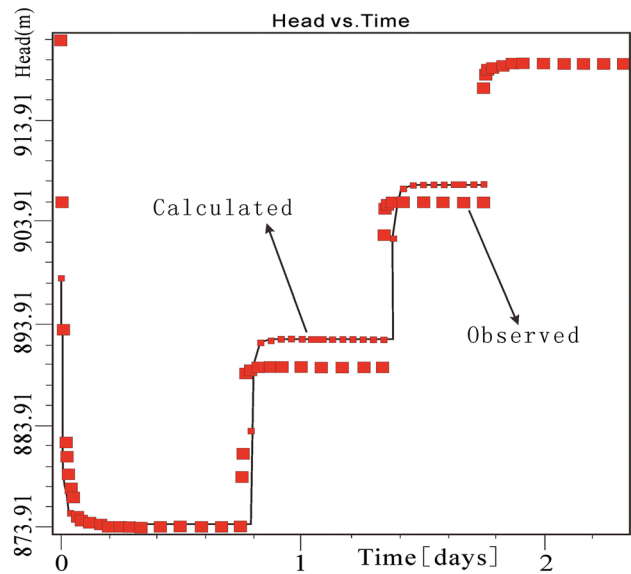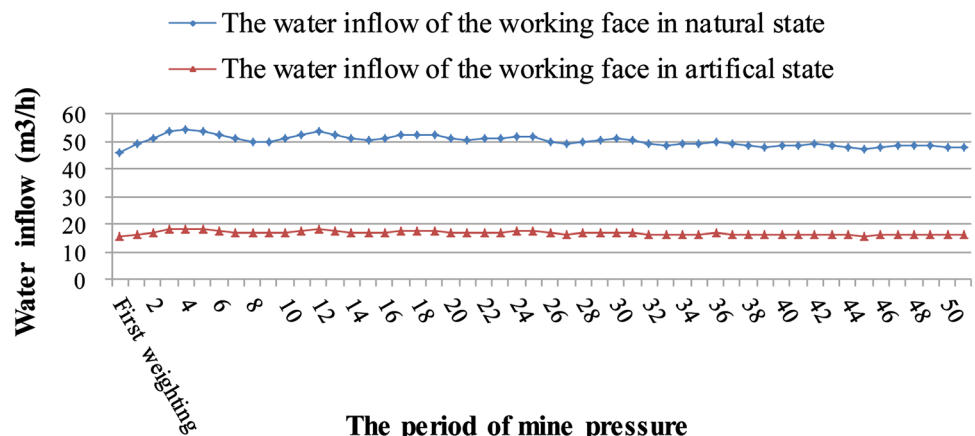

Fig. 9 The fitting graph for water level of pumping test

Fig. 10 Dynamic change of engineering inflow from 20,518 working face

the area, five main factors were chosen that influence aquifer water abundance: permeability coefficient, brittle-plasticity ratio, total core recovery, drilling fluid quantity, and aquifer thickness. The relative importance of each influential factor was calculated from coupling GIS with AHP, taking advantage of AHP's ability to combine qualitative and quantitative analyses. Finally, we used the information fusion function of GIS to superimpose the factors onto a map, and then used the results to evaluate the water abundance of the roof aquifer.

Borehole inflow data were used to verify and calibrate the calculated aquifer water abundance. First, borehole inflow data were used with GIS technology to produce a water inflow thematic map. Then, a trend comparison was made with the water abundance thematic map. Data from seven representative boreholes were used to verify the evaluation zoning. The water abundance zoning obtained from the calibrated model reflected the roof aquifer's water abundance in the mine very well. The evaluation thematic map of aquifer water abundance was superimposed onto the thematic map of roof crack safety evaluation to produce a comprehensive evaluation of water inflow (inrush) risk.

References

Booth CJ (1986) Strata-movement concepts and the hydrogeological impact of underground coal mining. Ground Water 24:507–515

Booth CJ, Bertsch L (1999) Groundwater geochemistry in shallow aquifers above longwall mines in Illinois, USA. Hydrogeol J 7:561–575

Booth CJ, Curtiss AM, Demaris PJ, Bauer RA (2000) Site-specific variation in the potentiometric response to subsidence above active longwall mining. Environ Eng Geosci 6:383–394

Dong S (2007). Current situation and prospect of coal mine geological guarantee technologies to improve safety and efficiency. Coal Sci Tech 35(3):1–5 **(in Chinese)**

Hill JG, Price DR (1983) The impact of deep mining on an overlying aquifer in western Pennsylvania. Ground Water Monit Rev 3:138–143

Hu W, Wang G (1997) Development of technique of controlling water hazard on coal mine. Coal Geol Explor 25:17–23 **(in Chinese)**

Islam MR, Hayashi D, Kamruzzaman AB (2009) Finite element modeling of stress distributions and problems for multi-slice longwall mining in Bangladesh, with special reference to the Barapukuria coal mine. Int J Coal Geol 78:91–109

Kim JM, Parizek RR, Elsworth D (1997) Evaluation of fully-coupled strata deformation and groundwater flow in response to longwall mining. Int J Rock Mech Min Sci 34:1187–1199

Liu Z, Yang B (2006) The use of numerical simulation methods to determine the water flowing fractured zone development of a high degree. Min Saf Environ Prot 33(5):16–19

Liu T, Shi L, Han J (2006) Hydraulic conductivity fracture zone height calculation. J China Coal Soc 31:93–96 **(in Chinese)**

Qian M, Miao X, Xu J (1996) Theoretical study of key stratum in ground control. J China Coal Soc 3:225–230 **(in Chinese)**

Rauch HW (1989) A summary of the ground water impacts from underground mine subsidence in the north central Appalachians. Ch 2. Coal Mine Subsidence Special Institute, Eastern Mineral Law Foundation, Pittsburgh, pp 201–231

Singh MM, Kendorski FS (1981) Strata disturbance prediction for mining beneath surface water and waste impoundments. In: Proc. 1st Conf on Ground Control in Mining, Morgantown, pp 76–88

State Council of the PRC (2014) Energy development strategy action plan (2014–2020). http://www.gov.cn/zhengce/content/2014-11/19/content_9222.htm. Accessed 7 June 2014

State Council of the PRC (2016) The opinions of about the coal industry solve the excess capacity to realize the difficulty relief development. http://www.gov.cn/zhengce/content/2016-02/05/content_5039686.htm. Accessed 1 Feb 2016

Wu Q (1995) The mine water management decision system of North China coal fields. China Coal Industry Publ House, Beijing **(in Chinese)**

Wu Q (2002) Prevention and treatment of mine water hazardous disaster. China University of Mining and Technology Press, Xuzhou **(in Chinese)**

Wu Q (2014) Progress, problems and prospects of prevention and control technology of mine water and reutilization in China. J China Coal Soc 39(5):795–805 **(in Chinese)**

Wu Q, Wang M (2006) Characterization of water bursting and discharge into underground mines with multi-layered groundwater flow systems in the North China Coal Basin. Hydrogeol J 14(6):882–893

Wu Q, Zhou W (2008) Prediction of inflow from overlying aquifers into coalmines: a case study in Jinggezhuang coal mine, Kailuan, China. Environ Geol 55:775–780

Wu Q, Zhao S, Sun W Liu S, Zeng Y (2013) Classification of the hydrogeological type of coal mine and analysis of its characteristics in China. J China Coal Soc 38(6):901–905 **(in Chinese)**

Wu Q, Liu Y, Zhou W, Li B, Zhao B, Liu S, Sun W, Zeng Y (2015a) Evaluation of water inrush vulnerability from aquifers overlying coal seams in the Menkeqing Coal Mine, China. Mine Water Environ 34(3):258–269

Wu Q, Liu Y, Luo L, Liu S, Sun W, Zeng Y (2015b) Quantitative evaluation and prediction of water inrush vulnerability from aquifers overlying coal seams in Donghuantuo Coal Mine, China. Environ Earth Sci 74(2):1429–1437

Xu J, Qian M (2000) Distinguishing method of position of overlying key stratum. J China Univ Min Technol 29(5):463–467 **(in Chinese)**

Xu Y, Li J, Liu S, Zhou L (2011) Computational formula of "two-zone" height of overlying strata and its adaptability analysis. Coal Min Technol 16(2):4–11 **(in Chinese)**

Xu D, Peng S, Xiang S, Liang M, Liu W (2016) The effects of caving of a coal mine's immediate roof on floor strata failure and water inrush. Mine Water Environ 35(3):337–349

Zeng Y, Liu S, Zhang W, Zhai Y. (2016a) Application of artificial neural network technology to predicting small faults and folds in coal seams, China. Sustain Water Resour Manag 2(2):175–181

Zeng Y, Wu Q, Liu S, Zhai Y, Zhang W, Liu Y (2016b) Vulnerability assessment of water bursting from Ordovician limestone into coal mines of China. Environ Earth Sci 75:1431. doi:10.1007/s12665-016-6239-4